

## PAPER

View Article Online  
View Journal | View IssueCite this: *RSC Mechanochem.*, 2025, 2, 482Received 23rd January 2025  
Accepted 16th March 2025

DOI: 10.1039/d5mr00016e

rsc.li/RSCMechanochem

# *In situ* Raman spectroscopy for comparing ball milling and resonant acoustic mixing in organic mechanosynthesis†

Leonarda Vugrin,<sup>ID ‡<sup>a</sup></sup> Christos Chatzigiannis,<sup>ID ‡<sup>b</sup></sup> Evelina Colacino<sup>ID \*<sup>b</sup></sup>  
and Ivan Halasz<sup>ID \*<sup>a</sup></sup>

By using *in situ* Raman spectroscopy for reaction monitoring, we compare ball milling (BM) and resonant acoustic mixing (RAM) in the preparation  $\alpha,\beta$ -unsaturated ketones (chalcones). RAM achieves similar transformations to BM, though adjustments in reaction conditions may be necessary due to different mixing regimes.

Mechanochemical processing techniques are becoming increasingly important in various industries for grinding, mixing, alloying and inducing chemical reactions among solid reagents and materials.<sup>1,2</sup> The mechanical energy driving such transformations arises from collisional and frictional interactions between the milling media and reaction material.<sup>3</sup> The former is most often achieved in ball milling (BM) devices, wherein the kinetic energy of milling balls activates and mixes powder materials to ultimately trigger and drive chemical reactions.<sup>4,5</sup> While BM is versatile and straight-forward, particularly suitable for laboratory-scale experiments, it may present certain drawbacks such as excessive heating<sup>6</sup> (mostly in the synthesis of hard materials), machine noise, and potential contamination due to the wear of the milling media<sup>7,8</sup> (especially when grinding media made of stainless steel or tungsten carbide are used). These issues are less relevant when softer organic materials are processed and can be further mitigated by the use of less aggressive chemicals, if available, the use of liquid additives, the use of more appropriate milling media, such as zirconium oxide, PTFE, or agate, and conducting the process at a lower operating speed.<sup>9</sup>

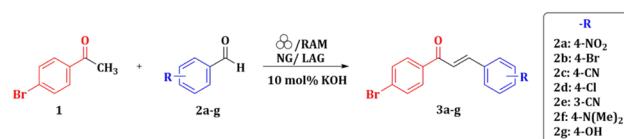
Material contamination is a common concern in mechanochemical methods, as collisions and friction are two key mechanical actions that may cause abrasion and introduce metal impurities.<sup>10</sup> Resonant acoustic mixing (RAM) has been recently proposed as a possible alternative to traditional ball-mills,<sup>11</sup> the milling balls not being necessarily required for promoting mechanochemical stress, generally leading to an efficient mixing process (which however, will be dependent on

the rheology of the mixture), by inducing bulk movements of the material inside the vessel.<sup>12</sup> RAM operates by vertical oscillations at a frequency of 60 Hz, occurring at variable accelerations, expressed commonly as a multiple of the Earth's force of gravity (*g*). Though the use of milling balls is eliminated in RAM, friction between the reactants and the vial walls remains and may still cause abrasion.<sup>13,14</sup> Oscillations in RAM contrasts the random and chaotic nature of energy transfer in BM and may allow for a simpler description of reaction kinetics and, possibly, more accurate prediction of reaction outcomes.<sup>15,16</sup>

The mechanistic and theoretical understanding of RAM-driven reactions remains unexplored and underdeveloped compared to those of BM.<sup>17</sup> To date, limited studies have applied *in situ* Raman spectroscopy in RAM.<sup>16</sup> Herein, the base-catalyzed Claisen–Schmidt condensation reaction between *p*-bromoacetophenone (**1**) and an array of different aromatic benzaldehydes (**2a–g**) was explored, with a particular focus on the reaction between **1** and *p*-nitrobenzaldehyde (**2a**), to compare the reaction rates and mechanisms of chalcone formation in BM and RAM by *in situ* Raman spectroscopy (Scheme 1).<sup>18,19</sup>

## Experimental part

Starting materials were milled at ambient temperature in an equimolar ratio at 30 Hz in a horizontal vibrating BM (with two



**Scheme 1** Mechanochemical synthesis of chalcones (**3a–g**) from **1** and differently substituted aromatic benzaldehydes **2a–g** with catalytic amount of potassium hydroxide (10 mol%) by BM and RAM.

<sup>a</sup>Ruder Bošković Institute, Bijenička c. 54, Zagreb, Croatia. E-mail: ivan.halasz@irb.hr

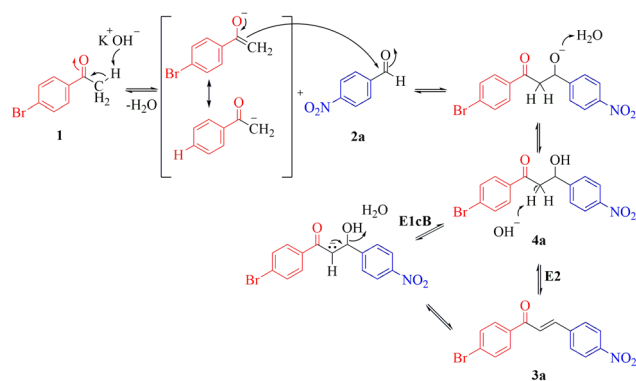
<sup>b</sup>ICGM, Univ Montpellier, CNRS, ENSCM, Montpellier, France. E-mail: evelina.colacino@umontpellier.fr

† Electronic supplementary information (ESI) available. See DOI: <https://doi.org/10.1039/d5mr00016e>

‡ Equal contribution.

1.4 g stainless steel (SS) balls, 7 mm diameter) or at the resonant frequency of 60 Hz (variation of acceleration from 80 g to 100 g) by RAM, in translucent poly(methyl methacrylate) jars (PMMA, either 14 mL or 7 mL internal volume). In RAM, the lack of milling media was compensated by filling the jar to 70–80% of its nominal volume to ensure proper mixing.<sup>20</sup> In both devices, the reaction progress was followed by real-time *in situ* Raman monitoring, while thin-layer chromatography, <sup>1</sup>H NMR spectroscopy and, if possible, Rietveld analysis of the powder diffraction patterns confirmed the formation of the target chalcones.

Initially performed in a well-established BM setup (horizontally vibrating ball mill), equipped with Raman *in situ* monitoring device, chalcone formation from **1** and **2a**, using



**Scheme 2** Proposed mechanism for the base-catalysed aldol condensation between **1** and **2a** proceeding through an aldol intermediate **4a**, which undergoes dehydration via two elimination pathways, with the E2 being generally more dominant in solution-phase chemistry.<sup>23</sup>

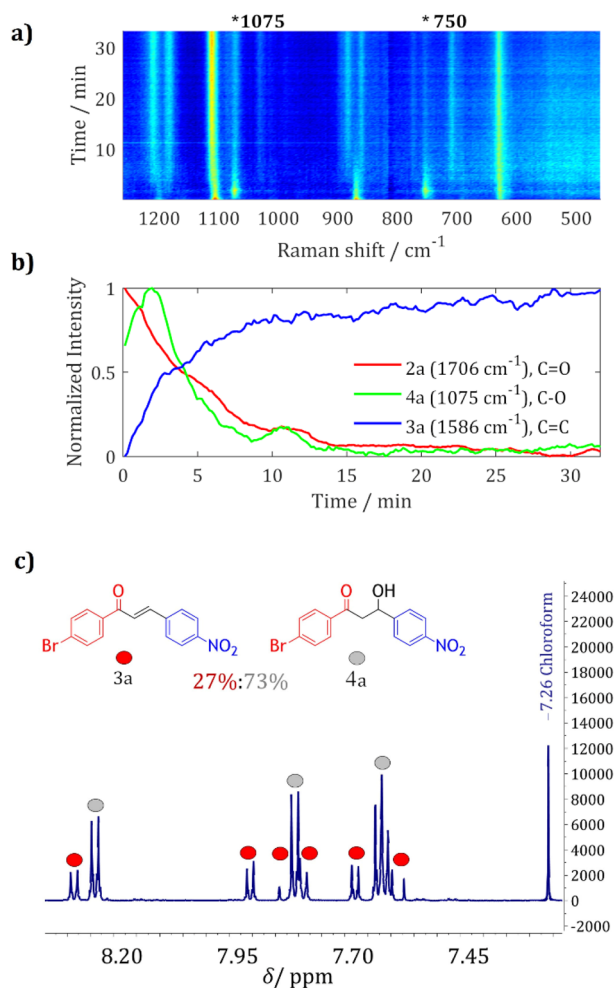


**Fig. 1** (a) Time-resolved 2D Raman plot of milling **1** and **2a** in a BM with denoted peaks that indicate the formation of intermediate specie. (b) Normalized intensity changes during time of characteristic bands for three components: **2a** (C=O bond vibration, decrease of Raman band at 1706 cm<sup>-1</sup>), the aldol intermediate **4a** peaking around first 2 min (new vibration bands in the region of C–O and C–H bonds vibrations at 1075 cm<sup>-1</sup> and 750 cm<sup>-1</sup>), and **3a** (C=C bond vibration, increase of Raman band at 1586 cm<sup>-1</sup>). (c) <sup>1</sup>H NMR spectrum (600 MHz, CDCl<sub>3</sub>) of the crude mixture collected after 5 min of milling at 30 Hz in a BM displayed with red circle corresponding to **3a** and the grey one to aldol **4a**.

a catalytic amount of KOH as the base, provided quality Raman spectra that enabled the identification of the desired product **3a**, as well as the expected aldol intermediate **4a** (Fig. 1). The formation of the aldol intermediate **4a** was followed by dehydration that established the conjugated C=C bond of the target chalcone (Scheme 2). The formation of **4a** has been well-documented in solution,<sup>21,22</sup> and for the benchmark reaction it was successfully observed by Raman spectroscopy showing its

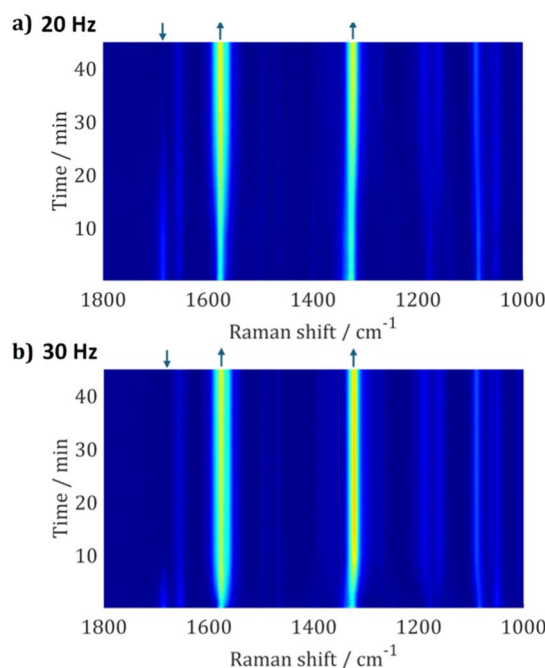


**Fig. 2** (a) 2D time-resolved Raman plot of monitoring the reaction between **1** and **2a** in a BM with 1 × 1.0 g SS milling ball (diameter 6 mm), during 40 min at: (a) 20 Hz and (b) 30 Hz milling frequency. In both plots, the downward arrow indicates the consumption of the reactant followed by the intensity decrease of band related to C=O functional group of **2a**, while the upward arrow points to the formation of the new C=C bond, product **3a**.



presence within 5 min of milling at 30 Hz. This was indicated by the emergence of new bands at  $1075\text{ cm}^{-1}$  and  $750\text{ cm}^{-1}$ , attributed to the vibrations of C–O and C–H bonds. In order to isolate the intermediate, milling was stopped after 3 min and **4a** was purified by column chromatography. Its structure was confirmed by solution  $^1\text{H}$  NMR analyses (Fig. S4 and S63†).

The next objective was to purposely slow down this quick reaction to ensure that the effects of milling parameters were well-understood prior to investigate the reaction by RAM activation. Thus, among the several mechanochemical parameters, our attention focused on investigating the influence of the ball mass and the milling frequency on the reaction progress. By reducing the number of SS milling balls from two bigger balls (mass 1.4 g each, 7 mm diameter) to one smaller ball (mass 1.0 g, 6 mm diameter), and by further lowering the milling frequency down to 20 Hz, the reaction was sufficiently slowed down to observe the formation of the aldol **4a** after *ca.* 10 min (Fig. 2, *cf.*, ESI, Fig. S64–S68†). This adjustment provided a baseline for mechanism comparison between the classical BM and the RAM method.

Following initial experiments by BM, the setup for *in situ* Raman measurements was adapted for use with a LabRAM II device (*cf.*, ESI†). During transfer from BM to RAM, diverse outcomes were observed depending on the reaction conditions

used. As per the method used by BM, stoichiometric amount of **1** and **2a** were mixed in neat grinding (NG) conditions first, during 60 min at 80 g.

In contrast to BM, only traces of the product **3a** could be observed under neat conditions by RAM, highlighting the fundamental differences in activation methods between systems with milling balls and without them.

Experiments conducted on a larger scale using a planetary ball mill (PM) with  $\text{ZrO}_2$  balls provided quantitative yield under neat grinding (Table 1, entry 5), further demonstrating the advantage of devices using milling media. Dry mixing in RAM led to the formation of distinct layers within the reaction vessel and an incomplete reaction (*cf.*, ESI†). In some cases, depending on the filling degree, the reaction stopped at the intermediate **4a**, as indicated by the light pink colour of the reaction mixture.

To evaluate the effect of the filling degree on the reaction course, experiments were conducted in two vessel sizes (7 mL and 14 mL nominal volumes), varying the filling degree by adjusting the amount of starting chemicals inside (1 mmol, 4 mmol, and 20 mmol). Trace amounts of product were observed at the 1 mmol scale (Table 1, entry 1), while a larger filling degree provided improved mixing. In the RAM device, managing the quantity of the material in the vessel was

Table 1 Comparative data for the preparation of **3a** by RAM, planetary ball mill (PM) and vibrating BM

Entry	EtOH, $\eta$ ( $\mu\text{L mg}^{-1}$ )	Activation technique	Speed	Time (min)	Filling degree (%)	NMR conversion (%)
1	—	RAM	80 g	60	4	Traces <sup>a,b</sup>
2	0.25	RAM	80 g	60	14	86 <sup>c</sup>
3	0.75	RAM	80 g	80	36	100 <sup>d</sup>
4	1.00	RAM	80 g	80	14	Traces <sup>e</sup>
5	—	PM	450 rpm	120	8	98 <sup>f</sup>
6	—	BM	30 Hz	120	1.8	97 <sup>g</sup>

<sup>a</sup> All the reactions were performed in the presence of KOH 10 mol% in PMMA jars. Reaction setup: PMMA jar (7 mL), 1 mmol scale. Too low amount of reaction material (brown powder). <sup>b</sup> PMMA jar (7 mL), 4 mmol scale. Slightly pink powder, aldol **4a** detected. <sup>c</sup> PMMA jar (7 mL), 4 mmol scale. <sup>d</sup> PMMA jar (14 mL), 20 mmol scale. <sup>e</sup> PMMA jar (7 mL), 4 mmol scale. Paste mixture, too high amount of liquid. <sup>f</sup>  $\text{ZrO}_2$  jar (12 mL), 4 mmol scale, 30  $\times$   $\text{ZrO}_2$  balls (mass 0.39 g each, 5 mm diameter). <sup>g</sup> PMMA jar (14 mL), 1 mmol scale, 2  $\times$  1.4 g (7 mm diameter) SS balls. NMR conversion was calculated according to the integral ratio of starting material ( $\delta_{\text{Ar-H}} = 7.82\text{ ppm}$ , d, 2H or  $\delta_{\text{CH}_3} = 2.59\text{ ppm}$ , s, 3H) and product ( $\delta_{\text{Ar-H}} = 8.30\text{ ppm}$ , d, 2H) recorded in  $\text{CDCl}_3$  (600 MHz).



essential, as its mixing relies on multiple mixing zones inside the vessel. This helps in preventing the formation of areas where the material is not effectively mixed, such as a too low amount of the reagents that may lead to poor contact between them.

The reaction in BM may be facilitated by more energetic impacts of milling balls, whereas the operation mechanism of RAM under dry conditions suggests that liquid-assisted grinding (LAG) might be necessary to achieve comparable reactivity.

The introduction of EtOH as a liquid additive was crucial to improve the reaction yield in RAM, its choice being based on its previous use in solution-based methods for aldol condensation.<sup>24–26</sup> The yield, however, was dependent on the amount of the added liquid, prompting us to screen different  $\eta$  values (0.05, 0.10, 0.15, 0.25, 0.75, 1.00  $\mu\text{L mg}^{-1}$ ). The best yield was achieved at  $\eta = 0.75 \mu\text{L mg}^{-1}$  (Table 1, entry 3). Increasing the amount of EtOH further to  $\eta = 1 \mu\text{L mg}^{-1}$  had a negative effect on the rheology of the reaction mixtures, that became pasty and gummy, hampering efficient mixing. This led to a significant decrease in reaction efficiency, yielding only trace amounts of the product (Table 1, entry 4).

These fluctuations presented difficulties in accurately monitoring the process with the setup for Raman measurements. A combination of mechanical and chemical optimization strategies was crucial for chalcone syntheses, while maintaining suitable conditions for Raman monitoring (Fig. 3, *cf.*, ESI†).

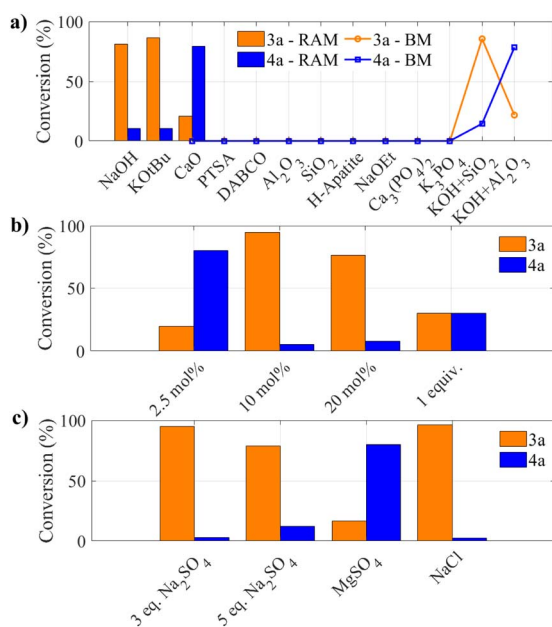


**Fig. 3** Comparative analysis of the effect of: (a) different bases in both RAM and BM, (b) molar ratios of KOH in RAM and (c) fillers (3 eq.) in RAM on reaction conversion of **3a** and **4a** during screening experiments. Standard experimental conditions were as follows: 10 mol% base, 1:1 molar ratio of starting materials, room temperature, 2 h reaction time, for BM: 1 mmol scale, PMMA jar (internal volume 14 mL),  $2 \times 1.4$  g SS balls (7 mm diameter each), 30 Hz, and RAM: 4 mmol scale, polypropylene vessel, LAG (EtOH) ( $\eta = 0.75 \mu\text{L mg}^{-1}$ ), 80 g. Differences between conditions are depicted on the x-axes.

Bases other than KOH were also tested, including sodium ethoxide, potassium carbonate, potassium and calcium phosphate, and hydroxyapatite, as well as the organic base 1,4-diazabicyclo[2.2.2]octane (DABCO). Surprisingly, none of them yielded the target product (Fig. 3a). Among all the bases tested, KOH consistently facilitated the reaction, making it the preferred base for use with both types of milling devices. The optimization of KOH quantity revealed that 10 mol% provided the best yield, while further increases in KOH led to a decrease in yield (Fig. 3b).

In order to improve conditions for Raman monitoring, we have considered the use of fillers. Thus,  $\text{Na}_2\text{SO}_4$  and NaCl were used as fillers and have demonstrated a positive effect on the reaction yield, while  $\text{MgSO}_4$  reduced the yield of **3a**, while improving the yield of **4a** (Fig. 3c, *cf.*, ESI†). These observations highlight the critical role fillers may have, demonstrating their ability not only to improve the rheology of the reaction mixture, but also to steer reaction selectivity. Beyond improving rheological properties, the presence of salt filler may have had additional influence to the reaction mechanism, particularly the elimination step. The cations may act as Lewis acids to shift the reaction mechanism to be more E1cB-like, due to Lewis-acid stabilisation of the conjugated base.<sup>27</sup> Quantitative conversion was obtained when using 3 equiv. of  $\text{Na}_2\text{SO}_4$  along with  $0.75 \mu\text{L mg}^{-1}$  of EtOH. These conditions were utilized to monitor the reaction using Raman spectroscopy and to compare the reaction mechanisms in two different mixing “environments”. Based on the collected Raman spectra, similar trends in reactant consumption and product formation were observed for BM and RAM (Fig. 4a and b).

In RAM, the reaction progresses rapidly under LAG, as evidenced by the sharp decline of the reactant signal and the quick formation of the intermediate **4a** and the final product **3a**. The reaction kinetics in RAM may be influenced by the stabilization of reaction intermediates due to the presence of Lewis acidic salt,  $\text{Na}_2\text{SO}_4$ , which may have favoured the E1cB elimination mechanism in comparison to BM, which proceeded without the salt filler and was possibly more E2-like.

Precise control over reaction parameters in RAM, such as filling degree, mixing intensity, and the potential use of liquid and solid additives, proved critical. These findings highlight the need for further optimization of reaction conditions to enhance the broader applicability of RAM in mechanochemical synthesis.

After real-time evaluation of the model system in both devices by Raman spectroscopy, the generality of the aldol condensation reaction was demonstrated on a series of aldehydes **2a–2g**, leading to a small library of chalcones **3a–3g** obtained in quantitative yields by: neat grinding in BM (30 Hz,  $2 \times 1.4$  g SS balls, 7 mm each) or liquid-assisted grinding in RAM (60 Hz,  $\eta$  (EtOH) =  $0.75 \mu\text{L mg}^{-1}$ , 3 equiv.  $\text{Na}_2\text{SO}_4$ ), with no traces of the corresponding intermediate aldols **4b–4g** (*cf.*, ESI, Table S9, S10, Fig. S54–S62, S82–S93 and S118–S125†). The observed structure-reactivity relationship aligns with the expected trend based on Hammett constants of the substituents on the phenyl ring, where electron-withdrawing groups enhance carbonyl electrophilicity and promote reactivity.<sup>28,29</sup> Notably, no



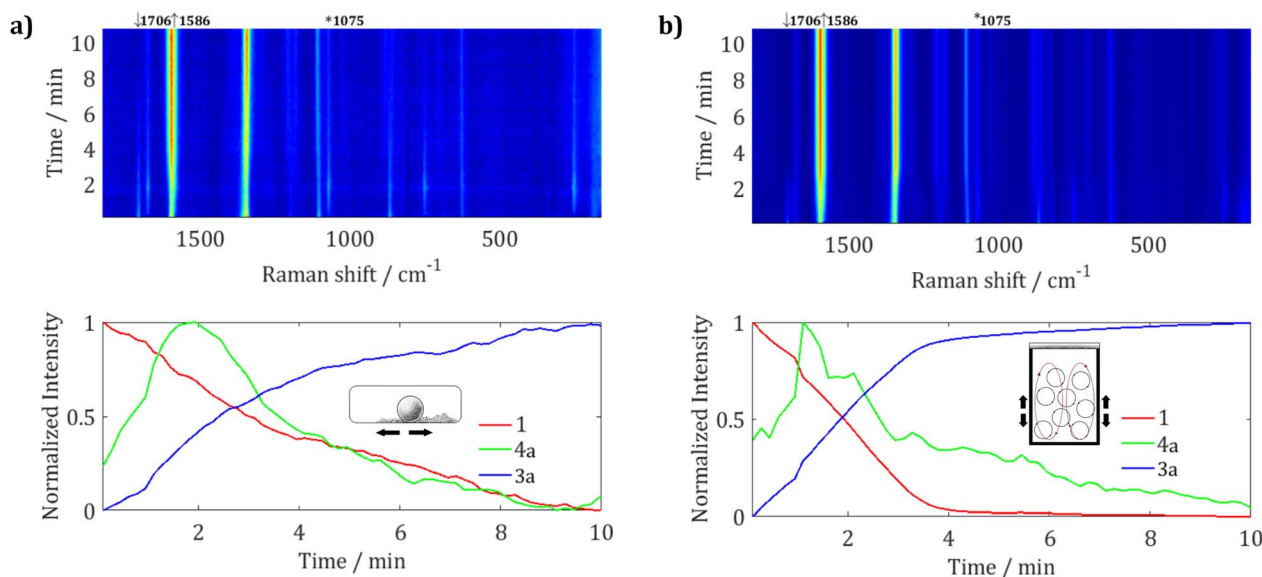


Fig. 4 Milling between **1** and **2a** in the presence of KOH (10 mol%) performed in two mechanochemical environments, (a) neat grinding (NG) in a vibrating BM and (b) in the presence of EtOH ( $\eta = 0.75 \mu\text{L mg}^{-1}$ ) and 3 equiv. of  $\text{Na}_2\text{SO}_4$  in RAM. (top) Time-resolved 2D Raman spectra showing the reaction progress with highlighted key Raman bands, indicating the formation of the aldol intermediate **4a** and the product **3a**. (bottom) Normalized intensity change over time for **1**, **4a**, **3a** of their most intensive characteristic Raman bands. Note that the Raman band of **4a** is of much lower intensity, which is not obvious due to normalisation.

product was obtained with **2g** (*p*-OH), while for **2f** (*p*-NMe<sub>2</sub>), the reaction mixture during suffered from eutectic melting, which impaired mixing. While we have not pursued to find the reason behind the lack of reaction with **2g**, we note that this was the only substrate that could act as a proton donor, which could have neutralised the KOH catalyst.

## Conclusion

The growing need to tailor mechanochemical processing methods to specific reactions requires deeper understanding of the relationships between different mechanical energy inputs. Here we have implemented *in situ* Raman spectroscopy as a tool to compare reaction conditions and mechanisms in BM and RAM. Our findings demonstrate that the milling balls in BM are crucial for delivering energy to the reactants, ensuring mechanochemical reactivity over a wide range of reaction conditions. In contrast, RAM appears to be more sensitive to adjustments in the reaction conditions, such as vessel filling degree and liquid additives that may be necessary to achieve comparable reaction rates. The reaction mechanisms may also be different and, surprisingly, different experimental conditions may be required to achieve the same mechanism by each of the methods. In RAM, the liquid serves not only to steer the reaction mechanism, but also to mitigate poor and non-uniform mixing, highlighting the importance of considering rheological properties of reaction mixtures during transfer from BM to RAM.

## Data availability

Data availability is being stated.

## Conflicts of interest

There are no conflicts to declare.

## Acknowledgements

We thank the French Embassy in Zagreb for funding a short-term student exchange for L. V. (Grant No. 01-1921/1-2023). I. H. and L. V. thank the Croatian Science Foundation for a financial support (grant No. IP-2020-02-1419). L. V. is supported by the Croatian Science Foundation (Grant No. 2795). E. C. is grateful to BetaInnov (<http://www.beta-innov.com>) for the permanent loan of planetary milling equipment.

## Notes and references

- 1 E. Colacino, M. Carta, G. Pia, A. Porcheddu, P. C. Ricci and F. Delogu, *ACS Omega*, 2018, **3**, 9196–9209.
- 2 H. J. Venables and J. I. Wells, *Drug Dev. Ind. Pharm.*, 2001, **27**, 599–612.
- 3 F. Delogu and L. Takacs, *J. Mater. Sci.*, 2018, **53**, 13331–13342.
- 4 M. Descamps and J. F. Willart, *Adv. Drug Delivery Rev.*, 2016, **100**, 51–66.
- 5 T. Kozawa, K. Fukuyama, K. Kushimoto, S. Ishihara, J. Kano, A. Kondo and M. Naito, *Sci. Rep.*, 2021, **11**, 210.
- 6 Y.-S. Kwon, K. B. Gerasimov and S.-K. Yoon, *J. Alloys Compd.*, 2002, **346**, 276–281.
- 7 J. Jablan, E. Marguá, L. Posavec, D. Klarić, D. Cincić, N. Galić and M. Jug, *J. Pharm. Biomed. Anal.*, 2024, **238**, 115855.
- 8 G. Štefanić, S. Krehula and I. Štefanić, *Dalton Trans.*, 2015, **44**, 18870–18881.



- 9 N. Fantozzi, J.-N. Volle, A. Porcheddu, D. Virieux, F. García and E. Colacino, *Chem. Soc. Rev.*, 2023, **52**, 6680–6714.
- 10 G. Štefanić, S. Krehula and I. Štefanić, *Chem. Commun.*, 2013, **49**, 9245–9247.
- 11 C. J. Wright, P. J. Wilkinson, S. E. Gaultier, D. Fossey, A. O. Burn and P. P. Gill, *Propellants, Explos., Pyrotech.*, 2022, **47**, e202100146.
- 12 L. Gonnet, T. H. Borchers, C. B. Lennox, J. Vainauskas, Y. Teoh, H. M. Titi, C. J. Barrett, S. G. Koenig, K. Nagapudi and T. Frišćić, *Faraday Discuss.*, 2023, **241**, 128–149.
- 13 F. Delogu and L. Takacs, *J. Mater. Sci.*, 2018, **53**, 13331–13342.
- 14 F. Delogu, *J. Phys.:Condens. Matter*, 2006, **18**, 8723–8736.
- 15 A. A. L. Michalchuk, K. S. Hope, S. R. Kennedy, M. V. Blanco, E. V. Boldyreva and C. R. Pulham, *Chem. Commun.*, 2018, **54**, 4033–4036.
- 16 C. B. Lennox, T. H. Borchers, L. Gonnet, C. J. Barrett, S. G. Koenig, K. Nagapudi and T. Frišćić, *Chem. Sci.*, 2023, **14**, 7475–7481.
- 17 S. Lukin, K. Užarević and I. Halasz, *Nat. Protoc.*, 2021, **16**, 3492–3521.
- 18 Y. N. Nayak, S. L. Gaonkar and M. Sabu, *J. Heterocycl. Chem.*, 2022, **60**, 1301–1325.
- 19 M. A. Shalaby, S. A. Rizk and A. M. Fahim, *Org. Biomol. Chem.*, 2023, **21**, 5317–5346.
- 20 L. Gonnet, C. B. Lennox, J.-L. Do, I. Malvestiti, S. G. Koenig, K. Nagapudi and T. Frišćić, *Angew. Chem., Int. Ed.*, 2022, **61**, e202115030.
- 21 A. M. Jawad, M. N. M. Salih, T. A. Helal, N. H. Obaid and N. M. Aljamali, *Int. J. Chem. Synth. Chem. React.*, 2019, **5**(1), 16–27.
- 22 D. Mulugeta, *Sci. J. Chem.*, 2022, **10**, 41–52.
- 23 F. A. Carey and R. J. Sundberg, *Advanced Organic Chemistry Part A*, New York, 5th edn. 2007, pp. 284–285.
- 24 T. V. Sreevidya, B. Narayana and H. S. Yathirajan, *Cent. Eur. J. Chem.*, 2010, **8**, 174–181.
- 25 K. Mezgebe, Y. Melaku and E. Mulugeta, *ACS Omega*, 2023, **8**, 19194–19211.
- 26 N. A. A. Elkanzi, H. Hrichi, R. A. Alolayan, W. Derafa, F. M. Zahou and R. B. Bakr, *ACS Omega*, 2022, **7**, 27769–27786.
- 27 T. Yan, Y. Sikai, D. Weili, W. Guangjun, G. Naijia and L. Landong, *Chin. J. Catal.*, 2021, **42**, 595–605.
- 28 L. Vugrin, M. Carta, F. Delogu and I. Halasz, *Chem. Commun.*, 2023, **59**, 1629–1632.
- 29 L. P. Hammett, *J. Am. Chem. Soc.*, 1937, **59**, 96–103.

